Effects of Mooring Line Failure on the Wave Frequency Responses of Truss Spar Platforms

M. A. W. Mohamed, O. A. Montasir, V. J. Kurian, M. S. Liew
Department of Civil Engineering, Universiti Teknologi PETRONAS
Bandar Seri Iskandar, Tronoh, Perak Darul Ridzuan, Malaysia

ABSTRACT

Experimental and numerical studies on a typical truss spar with intact and damaged mooring line conditions are presented. Physical model motions in surge, heave and pitch in addition to the mooring line tensions were measured. A MATLAB code named TRSPAR was developed for the dynamic analysis of truss spar. The numerical predictions agree very well with the measurements for the two structure conditions. Mooring line failure has shown insignificant effect on the wave frequency responses of the truss spar. However, for relatively low frequency waves, surge responses for mooring damage condition are lower than the corresponding intact mooring condition responses.

KEY WORDS: Truss spar; responses; mooring lines; waves; experiment; simulation.

INTRODUCTION

The challenging deepwater environment makes the traditional fixed offshore structures unsuitable. Therefore, alternative innovative platform concepts such as spar have been developed. In general, truss spar, which is the second generation, has low fabrication cost, less surge offset and less mooring line requirements compared to the first generation classic spar. In the late 1990s, development of truss spar concept advanced much with a large amount of research effort in model test (Prislin et al 1998, Troesch et al 2000), and theoretical study (Kim et al 1999, Luo et al 2001, Wang et al 2002).

Spar platform has six degrees of freedom. However, the dominant motions are only three; i.e., surge, heave and pitch. It has natural frequencies of motions far below the dominant ocean exciting wave forces frequencies; this is due to its large mass and relatively small restoring stiffness.

Mooring lines form an integral part of floating offshore structures. Many studies have been conducted on its effect on the structure motions. In general, methods of analysis of mooring line can be classified into two main categories known as quasi-static analysis and dynamic analysis. The main difference between these two methods is the effect of fluid mooring line interaction, which is considered only in the dynamic analysis. Under the assumption of the insignificance of the generated drag and inertia forces on the mooring line due to its motion, Ansari (1980) used the catenary equations for conducting static analysis for multi component mooring line. Under the same assumption, Agarwal and Jain (2003) developed an iterative numerical scheme that can be used for predicting the mooring line restoring force-excursion relationship which is required for solving the equation of motion.

Many studies considered the dynamic effects of the mooring line. These studies followed two methods. First, the semi-coupled dynamic analysis in which a separate program based on either finite element method or lumped mass method (Boom 1985) is required to predict mooring line tension. Second, the fully coupled analysis (Zhihuang 2000) in which the structure with its mooring lines was considered as a coupled structural system. In comparison with the quasi-static analysis and semi-coupled analysis, the fully coupled analysis is more accurate but it is computationally intensive.

A truss spar model of scaling factor 1:100, restrained by four mooring lines, was tested using regular waves in a wave basin 22 m long and 10 m wide with a water depth of 1.1 m. The experiments were performed for the model with intact mooring and mooring line failure conditions. The responses in surge, heave and pitch were measured. A MATLAB program named 'TRSPAR' was developed to determine the responses in these two situations. Time domain integration using Newmark Beta method was employed and the platform was modeled as a rigid body with three degrees of freedom restrained by mooring lines affecting the stiffness values. Hyperbolic extrapolation and the extended Morison equation for an inclined cylinder were used for simulating the sea state and for determining the dynamic force vector respectively. Added mass and damping were derived from hydrodynamic considerations.

The accuracy of TRSPAR in predicting the truss spar motions in the intact and damaged mooring conditions was validated by comparing the numerical results with the experimental measurements. To investigate the effect of mooring line failure on the wave frequency responses of the structure, comparisons between the results was made for the two structure situations.

FORMULATION

In consideration of the incident waves that are long crested and advancing in the *x*-direction, a spar is approximated by a rigid body of three degrees of freedom (surge, heave and pitch), it derives its static resistance from support systems (mooring lines, risers) and hydrostatic stiffness.

Two coordinate systems are employed in the analysis (see Fig.1), the space fixed coordinate system oxz and two dimensional local coordinate $G\zeta\eta$ which is fixed on the body with the origin at its center of gravity (CG). B is the center of buoyancy and F denotes fairlead.

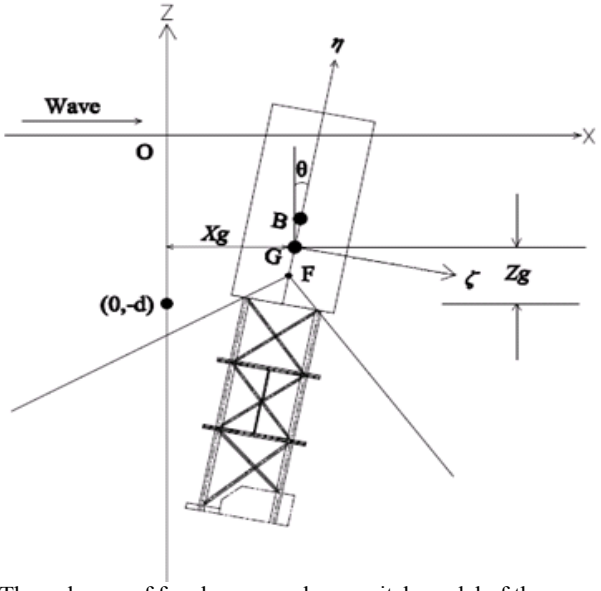

Fig.1 Three degree of freedom surge-heave-pitch model of the spa

The dynamic equations of the surge-heave-pitch motions of the spar are:

$$\{M\}\left[\frac{\partial^2 x_G}{\partial t^2}\right]+\{C\}\left[\frac{\partial x_G}{\partial t}\right]+\{K\}[x_G]=[F(t)] \qquad (1)$$

where $\{M\}$ is made up of body mass and added mass components as given in Eq. 2 and $\left[\frac{\partial^2 x_G}{\partial t^2}\right]$ is the structural acceleration vector. The resultant force can be defined as

$$\{M\}\left[\frac{\partial^2 x_G}{\partial t^2}\right]=\left\{\underbrace{\begin{bmatrix} m & 0 & 0\\ 0 & m & 0\\ 0 & 0 & I\end{bmatrix}}_{Mass\ matrix}+\underbrace{\begin{bmatrix} m_{11} & m_{12} & m_{13}\\ m_{21} & m_{22} & m_{23}\\ m_{31} & m_{32} & m_{33}\end{bmatrix}}_{Added\ mass\ matrix}\right\}\begin{bmatrix}\frac{\partial^2 x_G}{\partial t^2}\\ \frac{\partial^2 z_G}{\partial t^2}\\ \frac{\partial^2 \vartheta}{\partial t^2}\end{bmatrix} \qquad (2)$$

where m, I and ϑ denote body mass, mass moment of inertia about the y-axis and the pitch angle respectively. The added mass is determined by integrating the added mass from the bottom of the structure/member to the instantaneous surface elevation. The computations of added-mass forces and moments are as follows:

$$\begin{aligned}
m_{11} &= \int_{n_b}^{n_t} \rho\, C_m\, A.dn\, \cos\vartheta\, \cos\vartheta\\
m_{12} &= m_{21} = -\int_{n_b}^{n_t} \rho\, C_m\, A.dn\, \sin\vartheta\, \cos\vartheta\\
m_{13} &= m_{31} = \int_{n_b}^{n_t} \rho\, C_m\, A\, n.dn \cos\vartheta\\
m_{22} &= \int_{n_b}^{n_t} \rho\, C_m\, A.dn \sin\vartheta \sin\vartheta\\
m_{23} &= m_{32} = -\int_{n_b}^{n_t} \rho\, C_m\, A\, n.dn \sin\vartheta\\
m_{33} &= \int_{n_b}^{n_t} \rho\, C_m\, A\, n^2.dn
\end{aligned} \qquad (3)$$

where n_t and n_b are the top and the bottom of the structure respectively. A and dn stands for the structure cross-sectional area and small segment length along the local coordinate n.

$\{C\}\left[\frac{\partial x_G}{\partial t}\right]$ is the structure damping matrix multiply by the body velocity vector in the considered degrees of freedom. The resultant force can be defined as

$$\{C\}\left[\frac{\partial x_G}{\partial t}\right]=\begin{bmatrix} c_{11} & 0 & 0\\ 0 & c_{22} & 0\\ 0 & 0 & c_{33}\end{bmatrix}\begin{bmatrix}\frac{\partial x_G}{\partial t}\\ \frac{\partial z_G}{\partial t}\\ \frac{\partial \vartheta}{\partial t}\end{bmatrix} \qquad (4)$$

Damping sources can be identified as structural, radiation, wave drift and mooring lines. The significant contribution comes from the drag force on the truss spar when using Morison equation. Mooring lines damping is considered insignificant in this study. The structure damping of the system is small compared to the other forces. That is due to the low natural frequencies of the system in all degrees of freedom. The computations of the structure damping elements are as follows:

$$c_{11} = 2\,\xi_s\,\omega_{ns}\,m$$
$$c_{22} = 2\,\xi_h\,\omega_{nh}\,m \qquad (5)$$
$$c_{33} = 2\,\xi_p\,\omega_{np}\,I$$

where the subscripts *s*, *h* and *p* stand for surge, heave and pitch respectively, ξ is the damping ratio in the specified direction of motion and ω_n is the natural frequency of the system in the specified degree of freedom.

Wave drift damping can be added to the *C* matrix as

$$\{C\} = \begin{bmatrix} c_{11} + B_{11_{wd}} & 0 & -z_G \times B_{11_{wd}} \\ 0 & c_{22} & 0 \\ -z_G \times B_{11_{wd}} & 0 & c_{33} + z_G^2 \times B_{11_{wd}} \end{bmatrix} \qquad (6)$$

where z_G is z-coordinate of the center of gravity.

$$B_{11wd} = 2.6\,\rho\,R\,a^2\,\omega\,(kR)^2 \text{ , when } (kR)<1$$
$$= 2.6\,\rho\,R\,a^2\,\omega, \text{ otherwise.} \qquad (7)$$

where *a* is the wave amplitude and (*kR*) is the diffraction parameter in which *k* is the wave number and *R* is the structure radius.

In addition to the aforementioned damping, heave plates greatly increase the heave added mass and viscous damping as follows

$$F = \frac{1}{2}\rho\,U\left|U\right|L^2\,C_D + \rho\,\frac{\partial U}{\partial t}L^3\,C_A \qquad (8)$$

where C_D, C_A and *L* are drag, added mass coefficients for the heave plates and the heave plate length respectively. *U* and $\frac{\partial U}{\partial t}$ represent the velocity and acceleration respectively of the plate perpendicular to its plane.

$\{K\}[x_G]$ is the system stiffness matrix multiplied by displacement vector. The stiffness matrix is composed of two main components, hydrostatic and mooring line stiffness matrices. The mooring lines, which are represented here by linear massless springs attached at the spar fairleads, are the only source of stiffness in the direction of surge motion. The hydrostatic buoyancy force provides the heave restoring force. Both types of stiffness contribute to the pitch stiffness. The resultant restoring force can be defined as

$$\{K\}[x_G] = \left[\underbrace{\begin{bmatrix} 0 & 0 & 0 \\ 0 & k_2 & 0 \\ 0 & 0 & k_3 \end{bmatrix}}_{Hydrostatic} + \underbrace{\begin{bmatrix} k_x & 0 & k_x h_2 \\ 0 & 0 & 0 \\ k_x h_2 & 0 & k_x h_2^2 \end{bmatrix}}_{Mooring\ lines} \right] \begin{bmatrix} x_G \\ z_G \\ \vartheta \end{bmatrix} \qquad (9)$$

where

$k_2 = \pi\,\rho\,g\,(D/2)^2$

k_3 = buoyancy force × distance from G to B

k_x = horizontal spring stiffness

h_2 = distance from G to fairlead

ρ, *g* and *D* are the water density, gravity acceleration and structure diameter respectively.

In general, k_x is a nonlinear function of the structure displacements. Thus the solution process involves updating the *K* matrix for each new displacement.

The wave forces are decomposed into the normal force F_{EXn} and tangential force F_{Ext} as

$$\begin{Bmatrix} F_{EXn} \\ M_{EX} \end{Bmatrix} = \int_{-d_1}^{\varsigma(t)} \rho(1+C_m)A(n)a_n \begin{Bmatrix} 1 \\ n \end{Bmatrix} dn + \int_{-d_1}^{\varsigma(t)} \frac{1}{2}\rho C_D D\left|V_n\right|V_n \begin{Bmatrix} 1 \\ n \end{Bmatrix} dn + \int_{-d_1}^{\varsigma(t)} \rho C_m A(n) V_n \tau^T v\tau \begin{Bmatrix} 1 \\ n \end{Bmatrix} dn \qquad (10)$$

Where

$$a_n = \left|a - (a.\vec{\tau})\vec{\tau}\right|$$
$$V_n = \left|V - r_s^{\cdot} - ((V - r_s^{\cdot}).\vec{\tau})\vec{\tau}\right|$$
$$\tau = \begin{bmatrix} \sin\theta \\ \cos\theta \end{bmatrix}$$

C_m was the added mass coefficient, C_D the drag coefficient, V_n the relative normal velocity, and $\vec{\tau}$ the unit vector along the η axis. *a* and *V* were the wave particle acceleration and velocity respectively, and $r_s^{\cdot}$ was structure velocity. The last term in Eq. 10, describes Rainey's normal axial divergence correction in which the velocity gradient matrix was given by:

$$v = \frac{\partial(u, w)}{\partial(x, z)} \qquad (11)$$

The tangential force could be determined by integrating the hydrodynamic pressure on the bottom surface S_B.

$$F_{EXt} = \iint_{S_B} \left(\rho \frac{\partial \phi^{(1)}}{\partial t} + \frac{1}{2} \rho \left| \nabla \phi^{(1)} \right|^2 \right) . n_t \partial S \qquad (12)$$

where $\phi^{(1)}$ is the first potential of incident waves.

Forces F_{EXn} and F_{Ext} were transferred into spaced-fixed coordinate system *oxz* as:

$$\begin{Bmatrix} F_{EXx} \\ F_{EXz} \end{Bmatrix} = \begin{Bmatrix} \cos\theta & \sin\theta \\ -\sin\theta & \cos\theta \end{Bmatrix} \begin{Bmatrix} F_{EXn} \\ F_{EXt} \end{Bmatrix} \qquad (13)$$

The equation of motion (Eq. 1) was solved by an iterative procedure using unconditionally stable Newmark's Beta method.

EXPERIMENTAL STUDIES

The experimental studies have been conducted in the Universiti Teknologi PETRONAS (UTP) offshore laboratory. These experiments were performed for two structure cases:

Case 1: This case represents the truss spar with its intact mooring lines. The truss spar model was connected to the wave basin floor by four mooring lines as shown in Figs 2 – 3.

Case 2: The same model with its mooring line system was modified to account for mooring line failure condition. This modification was performed by relaxing the up-wave mooring lines to obtain the migration surge distance caused due to mooring line failure.

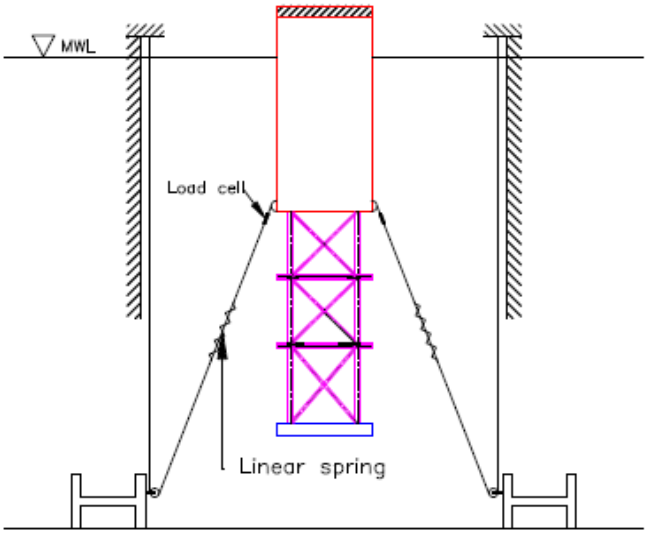

Fig.2 Sea keeping tests setup (side view)

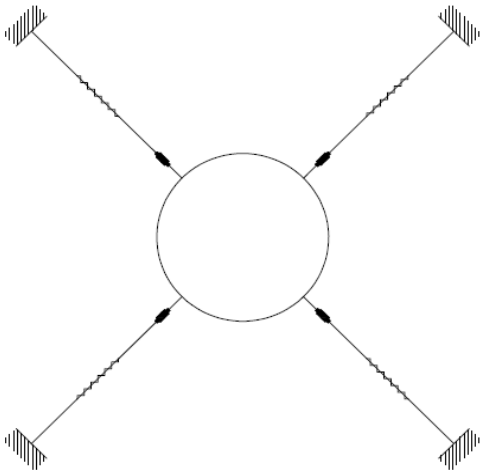

Fig.3 Model mooring line arrangement

Model Description

A truss spar model was made of steel plates to the scale of 1:100 according to the dimensions shown in Fig. 4. The constructed model undergoing tests is shown in Fig. 5. Table 1 shows the summary of the general structural data of the freely-floating truss spar (full scale). The model motions and the restraining mooring line tensions were measured by optical tracking system and load cells respectively.

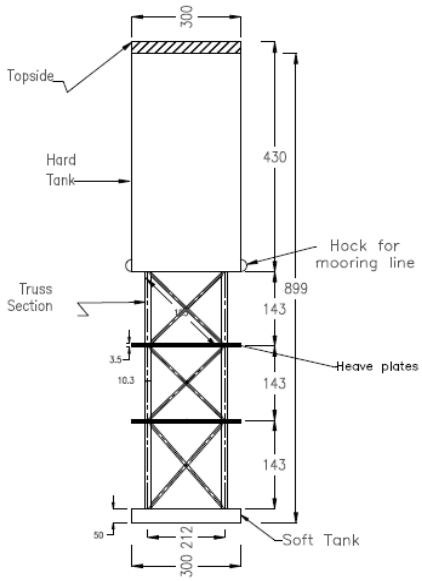

Fig.4 Truss spar model configuration (All dimensions are in mm)

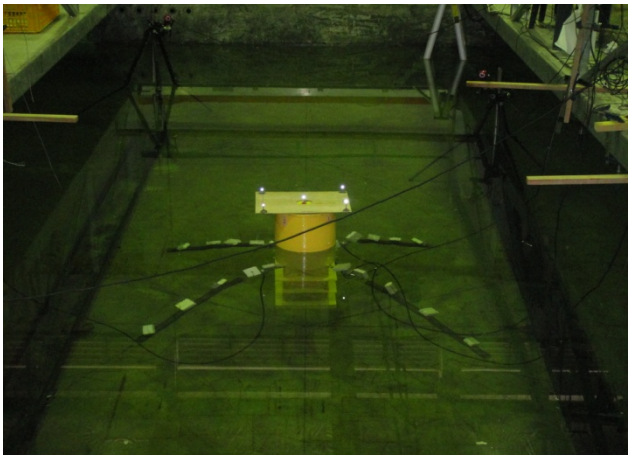

Fig.5 The truss spar model during tests

Table 1. The truss spar data (full scale)

Description		Value
Overall length (m)		90.9
Draft (m)		70.4
Vertical center of gravity from the keel (m)		43.5
Vertical center of buoyancy from the keel (m)		48
Mass (ton)	Hard tank	8.5×10^3
	Truss members	1.6×10^3
	Heave plates	4.7×10^3
	Soft tank	3.3×10^3
	Other weights	2.86×10^3
	Total	20.96×10^3
Pitch radius of gyration (m)		2.686×10^6
Water depth (m)		110

Mooring Line System

Modeling of platforms involves modeling both the floating structure and the mooring system. Due to the limitations of the wave basin, it is common to model the mooring lines as springs and their effects are incorporated in the equation of motion by obtaining the static offset test results. The same procedure has been adopted in this study.

In the sea keeping tests, the cables with soft springs, as shown in Figs 2 - 3, were used as mooring lines. Load cells were connected between the model and the spring for measuring mooring line tension in the fairlead. Small pieces of foam were attached to the springs and to the load cells to make them neutrally buoyant in water. It should be noted that the restraining system was pre-tensioned through pulley system and clamped in a way to ensure that no slacking of the wire occurred during the tests.

Experimental Programs

Quasi static test. Static offset tests were carried out, for the two structure cases, to determine the mooring system stiffness. Load cells were attached to the up and down stream mooring lines. The model was pulled horizontally from the downstream side. Accordingly, the horizontal movements and the readings from the load cells were recorded simultaneously. Using this data, the force-displacement relationship was constructed. The measurements were taken for every 4 m (full scale) horizontal displacement increment.

Free-decay test. In order to design the model with relatively low natural frequencies in all degrees of freedom, soft springs with 8.2 N/m stiffness (model scale) were used in the experiments to represent the mooring lines system. Free decay tests were conducted for Cases 1 and 2. The purpose of these tests was to predict the natural frequencies of the system in different conditions. The structural damping of the system was obtained by

$$\varsigma \cong \frac{1}{2\pi}.\ln\left[\frac{a_i}{a_{i+1}}\right] \qquad (14)$$

where a_i and a_{i+1} are the motion crest amplitude of the i^{th} and the $(i+1)^{th}$ cycles respectively.

Sea-keeping tests. For evaluating the sea-keeping characteristics of the model, it was tested for set of regular waves. For measurements of the generated wave profiles, four wave probes were placed in the wave basin. Two were in front of the model and the other two at the back of the model. These remained in place during the whole experiments. The acquired data includes the model three DOF motions, mooring loads and the environmental variables (wave height and wave period).

The tests for regular waves were carried out for the range of the dominant wave frequencies. Table 2 summarizes the target and measured regular waves for the two structural cases. The test duration for each run was thirty minutes (full scale).

RESULTS AND DISSCUSSIONS

The experimental studies associated with the numerical simulations were made for a typical truss spar platform with intact and mooring line damage conditions. In this study, an assumption was made that the model follows the Froude's law of similitude.

The numerical predictions were compared with the corresponding model test measurements (full scale) in terms of RAO for regular waves shown in Table 2. In order to compare between the numerical and experimental results, mooring line stiffness, which was found from the static offset test, was used as input in the numerical model.

Table 2. Wave height and period of regular waves used for testing

Drive signal	Wave height (m)		Wave period (s)	
	Target	Measured	Target	Measured
RG1	4	3.8	6	6
RG2	4	3.7	7	7
RG3	5	4.8	8	8
RG4	6	5.9	9	9
RG5	7	6.85	10	10
RG6	8	7.9	12	12
RG7	9	8.85	14	14
RG8	10/8*	10/8*	16	16
RG9	11/8*	11.1/8*	18	18
RG10	12/8*	12.2/8*	20	20

*This wave height was used for mooring line damage condition

Mooring Line Stiffness

In order to design the model with relatively low natural frequencies in all degrees of freedom, soft springs with 8.2 N/m stiffness (model scale) were used in the experiments to represent the mooring lines system.

Fig. 6 shows the comparison between the static offset test results for the structure with intact and mooring line failure conditions. It was shown that, mooring line failure significantly reduced the mooring line stiffness. In addition, mooring line failure gave -35 KN (full scale) restoring force to the system at 0 m horizontal offset due to the unbalance between the resultant mooring line tensions at each sides. This restoring force caused the initial horizontal excursion for the structure.

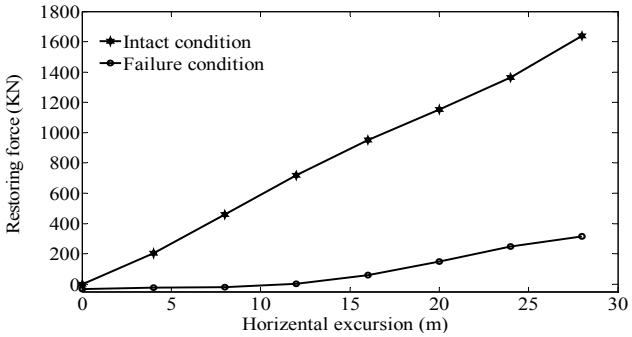

Fig.6 Static offset test results for cases 1 and 2.

Free-Decay Results

Comparisons between the surge free-decay physical measurements and simulations for cases 1 and 2 are shown in Fig. 7 and Fig. 8 respectively. The numerical simulations gave good results when compared to the test results. Table 3 shows that the calculated natural periods and damping ratios (using Eq. (14)) were closed to the measurements.

Table 3 shows that failure of mooring line affected the surge motion by increasing the corresponding natural period. This is because of decreasing mooring line stiffness, which is the only stiffness source of the system in the surge direction

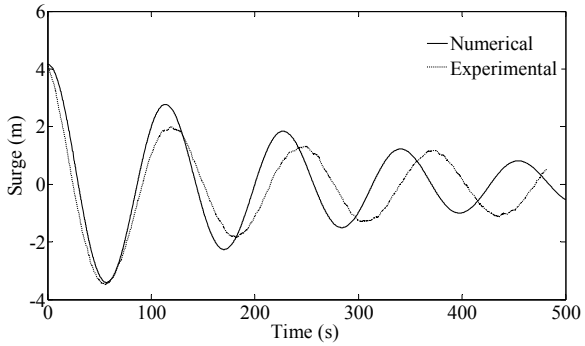

Fig. 7 Surge free decay results for case 1.

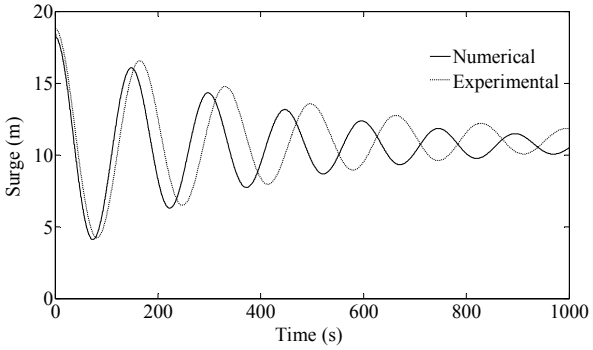

Fig. 8 Surge free decay results for case 2.

Table 3. Comparison of surge natural periods and damping ratios

Structure cases	Natural periods (s)		Damping ratio (%)	
	Simulated	Measured	Simulated	Measured
Case 1	114.5	121.25	6.6	6.9
Case 2	150	158	1.3	1.41

Intact Mooring Line Condition

The responses of the truss spar prototype were determined numerically using the structure dimensions, properties, draft and the generated wave characteristics (full scale) as input and the results were compared with the corresponding experimental data.

As shown in Figs. 9 - 11, the prototype RAOs for surge, heave and pitch of the numerical analysis were compared with the experimental processed results for regular waves, which covered the dominant ocean wave frequencies (Table 2). The simulated results agreed well with the measurements. The trend of the surge RAO agreed well with the measured values with maximum difference of 25%. The numerical heave RAOs agreed very well with the experiments. For the pitch RAO, the simulation results followed the same trend as experimental results with maximum difference of 16.7%. From these comparisons, it could be observed that the numerical model is capable to accurately predict the truss spar responses in the wave frequency range.

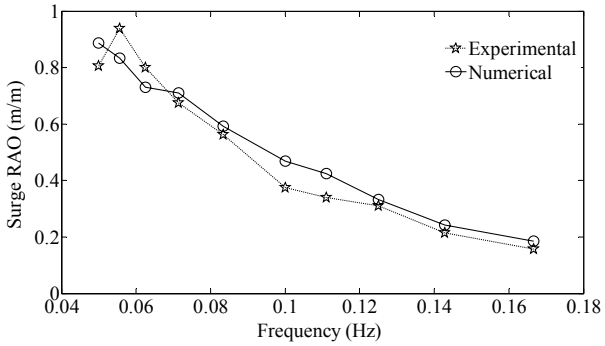

Fig.9 Surge RAOs

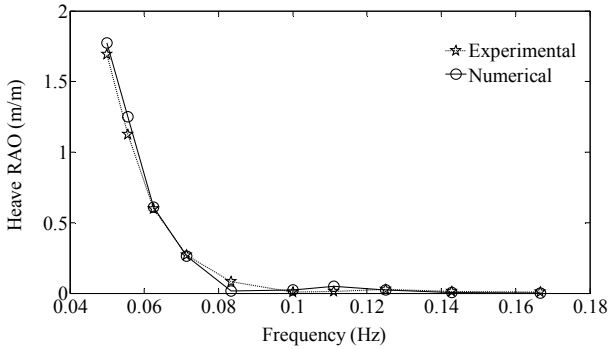

Fig.10 Heave RAOs

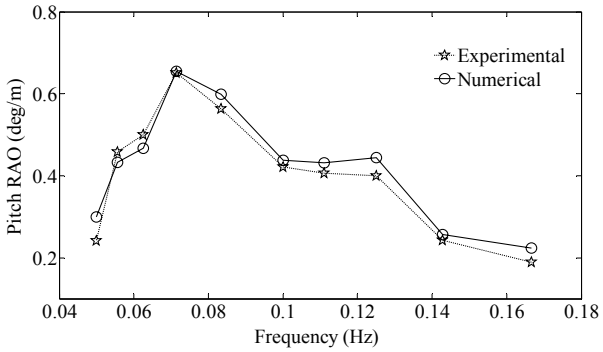

Fig.11 Pitch RAOs

Mooring Line Damage Condition

An attempt was made to investigate the effect of the mooring line failure phenomena on the motion characteristics of truss spar platform. This was made by relaxing the up-wave mooring lines and conducting the same sea keeping tests.

Figs 12 – 14 show the RAOs for surge, heave and pitch respectively for the structure under mooring line failure condition. For these three degrees of freedom, the numerical predictions agreed well with the experimental measurements. As the aim of this particular study is to examine the effect of the mooring line failure on the truss spar motion characteristics, the RAOs of the three degrees of freedom in the two cases are compared. For surge motion (Fig. 9 and Fig. 12), the general performance of the prototype is almost same. However, for relatively low frequency regular waves, surge RAOs under mooring line failure is lower than the normal case. This is because of the migration distance, which caused an increase in the mooring line stiffness of the structure in this case.

For heave (Fig. 10 and Fig. 13) and pitch (Fig. 11 and Fig. 14) motions, the two cases are almost similar since the mooring line stiffness has insignificant effect on these motions.

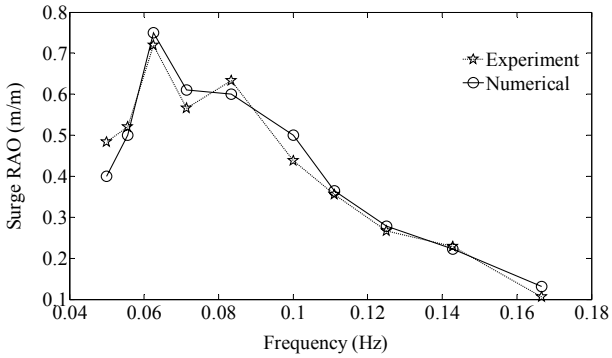

Fig.12 Surge RAOs

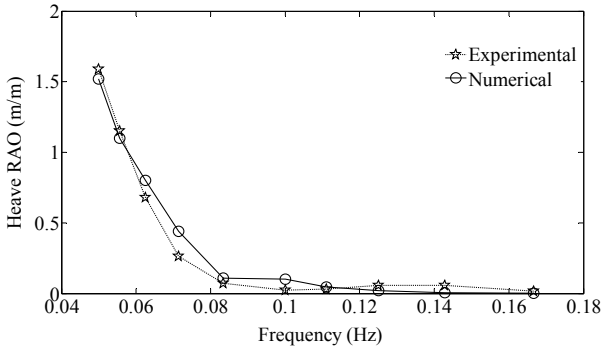

Fig.13 Heave RAOs

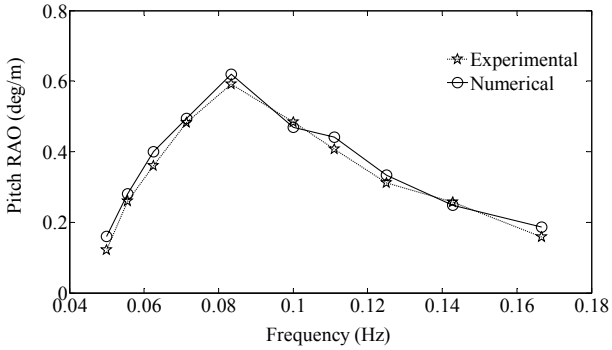

Fig.14 Pitch RAOs

Mooring Line Failure Mechanism

As shown earlier, surge motion was most affected by the mooring line failure. Therefore, surge responses due to RG4 were selected to present the transition process from intact to mooring line failure condition.

The experimental surge measurements in the two conditions are shown in Fig. 15 and Fig. 16 while the whole process, which simulated the conversion from the intact mooring condition to the failure condition, is shown in Fig. 17. In the simulation, the normal condition was considered up to 1000 s and then the mooring line failure was assumed.

As could be seen, the effect of mooring line failure on surge motion was well predicted by the numerical model with small differences in the mean position of the structure in the two conditions. In the intact mooring condition, the numerical code gave 0.93 m mean position while the measurements showed 1.6 m. In the failure case, the mean position was 15.3 m and 16.4 m for the predictions and measurements respectively. These differences in the mean position are due to using equations proposed by Weggel (1996) to calculate the mean drift forces in the simulation rather than measuring these forces in the experiments.

At this point, it is interesting to recall Fig. 6, which shows -35 KN mooring line restoring force at 0 m offset. This force affected the migration distance shown in Fig. 15. In addition to the migration distance effect, Fig. 15 shows transient surge response occurring immediately after failure. This transient response is very important in the analysis and design of mooring lines and risers.

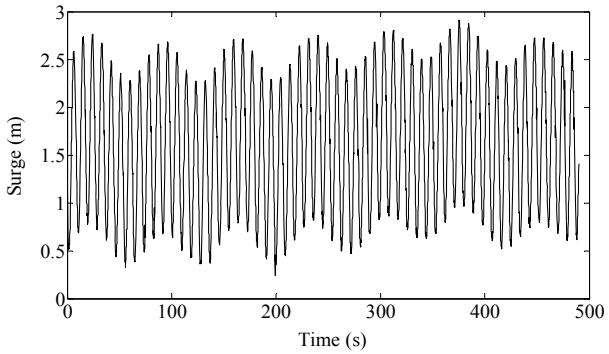

Fig.15 Surge time series for case 1 (experiment measurements)

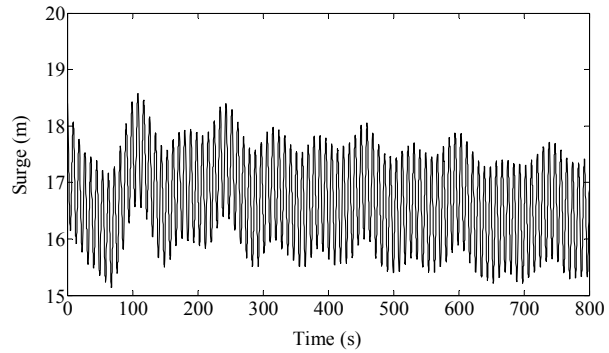

Fig.16 Surge time series for case 2 (experiment measurements)

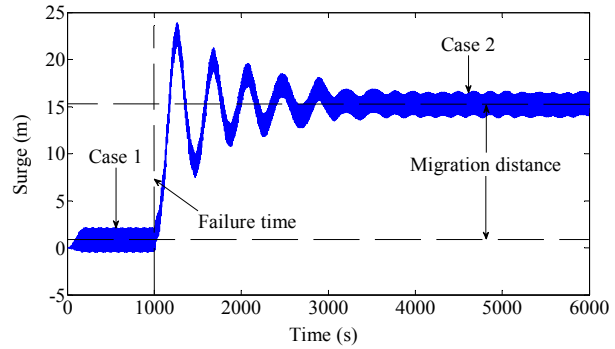

Fig.17 Surge time series for failure condition (numerical predictions)

CONCLUSIONS

1. The numerical model "TRSPAR" developed for assessment of the truss spar wave frequency responses was able to predict the platform motions due to regular waves obtaining good agreement with experimental results. This was verified in the case of intact mooring and mooring lines failure conditions.

2. Mooring line failure affected surge responses more than heave and pitch responses. Mooring line failure surge RAOs were almost same as intact mooring response RAOs except for relatively low frequency wave components where mooring damage condition gave lower results.

3. The major contribution of mooring line failure to the structure was causing the migration surge distance. This migration distance occurred due to the unbalanced upper and downstream mooring line forces. In addition, a noticeable transient surge response followed the failure.

REFERENCES

A. K. Agarwal and A. K. Jain (2003), "Dynamic behavior of offshore spar platforms under regular sea waves," Ocean Engineering Journal, pp. 487-516.

B. B. Mekha, et al. (1995), "Nonlinear response of spar in deep water: Different hydrodynamic and structural models," *Proc 5th Int Offshore and Polar Eng Conf*, ISOPE, The Hague, The Netherlands.

Cao, P.M., (1996), "Slow Motion Responses of Compliant Offshore Structures," MS Thesis, Ocean Engineering Program, Civil Eng. Department, Texas A&M University, College Station, Texas.

Chakrabati, S.K., (2001), "Hydrodynamics of Offshore Structures," Computational Mechanics Publications, Southampton, Boston.

D. Weggel (1996), "Nonlinear dynamic response of large diameter offshore structures," *PhD Thesis*, University of Texas, Austin, Tx.

H. J. J. v. d. Boom (1985), "Dynamic behaviour of mooring lines," *Proc 4th Int Conf on Behaviour of Offshore Structures, BOSS'85*, Delft, The Netherlands, pp. 359–368.

K. A. Ansari (1980), "Mooring with multicomponent cable systems," *Journal of Energy Resources Technology*, Trans. ASME, Vol. 102, pp 62-69.

Kim, MH, Ran, R, Zheng, W, Bhat, S, and Beynet, P (1999). "Hull/Mooring Coupled Dynamic Analysis of a Truss Spar in Time Domain," *Proc 9th Int Offshore and Polar Eng Conf*, ISOPE, Brest, France.

Luo, YH, Lu, R, Wang, J, and Berg S (2001). "Time-Domain Fatigue Analysis for Critical Connections of Truss Spar," *Proc 11th Int Offshore and Polar Eng Conf*, ISOPE, Stavanger, Vol 1, pp 362-368.

Prislin, I, Belvins, RD, and Halkyard, JE (1998). "Viscous Damping and Added Mass of Solid Square Plates," *Proc 17th Int Conf on Offshore Mechanics and Arcitic Eng*, OMAE, Lisbon, Portugal.

Troesch, AW, Perlin, M, and He, H (2000). "Hydrodynamics of Thin Plates," *Joint Industry Report*, U Michigan, Dept Naval Architecture and Marine Engineering, Ann Arbor.

Wang, J, Luo, YH, and Lu, R (2002), "Truss Spar Structural Design for West Africa Environment," *Proc 21st Int Conf on Offshore Mechanics and Arcitic Eng,* OMAE, Oslo, Norway.

Zhihuang, R (2000), "Coupled Dynamic analysis of floating structures in waves and currents," *PhD Thesis*, Office of Graduate Studies, Texas A&M University, Texas